

**Synthetic analogues of FTY720 differentially regulate
pulmonary vascular permeability *in vivo* and *in vitro***

SM Camp, R Bittman, ET Chiang, L Moreno-Vinasco, T Mirzapioazova, S Sammani, X
Lu, C Sun, M Harbeck, M Roe, V Natarajan, JGN Garcia, SM Dudek*

Section of Pulmonary and Critical Care Medicine, Department of Medicine, University of
Chicago, Chicago, Illinois (S.M.C, E.T.C, L.M.V., T.M., S.S., M.H., M.R., V.N., J.G.N.G.,
S.M.D.); Department of Chemistry and Biochemistry, Queens College of The City
University of New York, Flushing, New York (R.B., X.L., C.S.)

RUNNING TITLE PAGE

Running title: FTY720 analogues alter vascular permeability

***Corresponding Author:**

Steven M. Dudek, MD
Section of Pulmonary & Critical Care Medicine
Department of Medicine
University of Chicago
5841 South Maryland Ave.
Chicago, IL 60637
Phone = 773 834 2390
Fax = 773 702 6500
Email = sdudek@medicine.bsd.uchicago.edu

Text pages: 39

Tables: 1

Figures: 8

References: 40

Abstract: 248 Words

Introduction: 770 Words

Discussion: 1500 Words

Abbreviations: acute lung injury (ALI); acute respiratory distress syndrome (ARDS); bronchoalveolar lavage (BAL); endothelial cell (EC); human pulmonary artery endothelial cells (HPAEC); lipopolysaccharide (LPS); methyl- β -cyclodextrin (M β CD); myeloperoxidase (MPO); myosin light chain (MLC); pertussis toxin (PTX); sphingosine 1-phosphate (S1P); S1P₁ receptor (S1P₁R); transendothelial electrical resistance (TER); white blood cells (WBC)

Recommended Section Assignment: GI, Hepatic, Pulmonary, and Renal

ABSTRACT

Novel therapies are needed to address the vascular endothelial cell (EC) barrier disruption that occurs in inflammatory diseases such as acute lung injury (ALI). We previously demonstrated the potent barrier-enhancing effects of both sphingosine 1-phosphate (S1P) and the structurally similar compound FTY720 in inflammatory lung injury. In this study, we examined the therapeutic potential of several novel FTY720 analogues to reduce vascular leak. Similar to S1P and FTY720, the (R)- and (S)-enantiomers of FTY720 phosphonate and enephosphonate analogues produce sustained EC barrier enhancement *in vitro*, as seen by increases in transendothelial electrical resistance (TER). In contrast, the (R)- and (S)-enantiomers of FTY720 regioisomeric analogues disrupt EC barrier integrity in a dose-dependent manner. Barrier-enhancing FTY720 analogues demonstrate a wider protective concentration range *in vitro* (1 μ M to 50 μ M) and greater potency than either S1P or FTY720. In contrast to FTY720-induced EC barrier enhancement, S1P and the FTY720 analogues dramatically increase TER within minutes in association with cortical actin ring formation. Unlike S1P, these FTY720 analogues exhibit differential phosphorylation effects without altering the intracellular calcium level. Inhibitor studies indicate that barrier enhancement by these analogues involves signaling via G_i-coupled receptors, tyrosine kinases, and lipid rafts. Consistent with these *in vitro* responses, the (S)-phosphonate analogue of FTY720 significantly reduces multiple indices of alveolar and vascular permeability in a lipopolysaccharide-mediated murine model of ALI (without significant alterations in leukocyte counts). These results demonstrate the capacity for

JPET #153544

FTY720 analogues to significantly decrease pulmonary vascular leakage and inflammation *in vitro* and *in vivo*.

INTRODUCTION

Sustained vascular barrier leak, a marked characteristic of acute inflammatory diseases such as acute lung injury (ALI) and sepsis, contributes to the high mortality of these conditions. Disruption of the pulmonary vascular endothelial cell (EC) monolayer in the lung microcirculation results in flooding of interstitial and alveolar compartments with fluid, protein, and inflammatory cells resulting in respiratory failure (Dudek and Garcia, 2001). Specific therapies that prevent or reverse inflammation-mediated vascular barrier leak are lacking (Wheeler and Bernard, 2007). We have previously demonstrated the potent barrier-enhancing properties of sphingosine 1-phosphate (S1P), a platelet-derived sphingolipid that rapidly induces EC cytoskeletal rearrangements leading to augmented EC monolayer integrity (Garcia et al., 2001). Through ligation of the Gi-coupled S1P₁ receptor (S1P₁R), S1P initiates a series of downstream events, including Rac activation, cortactin translocation, peripheral myosin light chain (MLC) phosphorylation, and focal adhesion rearrangement, culminating in enhancement of the EC cortical actin ring, improved cell–cell and cell–matrix interactions, and increased barrier function *in vitro* (Garcia et al., 2001; Shikata et al., 2003; Dudek et al., 2004). We have also shown the *in vivo* capacity for S1P to attenuate lipopolysaccharide (LPS)-induced murine and canine models of sepsis and ALI (McVerry et al., 2004; Peng et al., 2004), supporting the potential therapeutic utility of this compound in inflammatory states.

Despite this impressive potential, S1P is an endogenous compound that produces a myriad of effects, including several that will limit its usefulness in patients.

For example, although intravascular administration of S1P protects against ALI, intratracheal administration can conversely produce pulmonary edema through disruption of the epithelial barrier via ligation of the S1P₃ receptor (S1P₃R) (Gon et al., 2005). Even in the vasculature, high concentrations of S1P (> 10 μM) can disrupt EC monolayer integrity *in vitro* through ligation of the S1P₃R and subsequent Rho activation, suggesting a limited therapeutic window for S1P's barrier enhancing properties. S1P also exhibits well-described cardiac toxicity (primarily bradycardia) through activation of S1P₃R in the heart (Forrest et al., 2004; Hale et al., 2004a). Finally, S1P can stimulate contraction of human airway smooth muscle cells (Rosenfeldt et al., 2003) and worsens airway hyperresponsiveness in mice (Roviezzo et al., 2007), suggesting a potential for S1P to exacerbate airway obstruction in asthmatics.

Given these limitations, there has been considerable interest in the biologic effects of the structurally similar compound, FTY720 (2-amino-2-(2-[4-octylphenyl]ethyl)-1,3-propanediol) (FTY720), which exhibits potent barrier-enhancing properties both *in vitro* and *in vivo* (Sanchez et al., 2003; Peng et al., 2004; Dudek et al., 2007). FTY720 has significant clinical interest as an immunosuppressive agent and has demonstrated efficacy in patients with relapsing multiple sclerosis (Kappos et al., 2006) and in models of leukemia (Neviani et al., 2007). It is currently being evaluated in Phase III clinical trials (Brinkmann et al., 2004; Mansoor and Melendez, 2008) and is, therefore, a potential future therapeutic option for inflammatory lung disease. Our prior *in vitro* studies demonstrate that FTY720 potently enhances EC barrier function, at least in part, via a novel S1P₁R-independent mechanism that involves an alternative G_i-coupled receptor (Dudek et al., 2007). We have also reported that a single intraperitoneal

injection of FTY720 significantly attenuated murine pulmonary injury measured 24 h after LPS administration (Peng et al., 2004).

However, similar to S1P, FTY720 has properties that may limit its therapeutic utility in patients with ALI. Its effectiveness as an immunosuppressant is related to its ability to induce lymphopenia via downregulation of lymphocyte S1P₁R signaling (Kovarik et al., 2004; Matloubian et al., 2004), but this effect may be detrimental in patients with ALI, many of whom have sepsis or infection as a triggering event (Wheeler and Bernard, 2007). Moreover, FTY720 induces bradycardia through similar S1P₃R-related mechanisms as S1P in both animals and patients (Brown et al., 2007), which may worsen the hemodynamic instability present in many ALI patients. Finally, in a recent multiple sclerosis clinical trial (Kappos et al., 2006), FTY720 significantly increased rates of dyspnea and decreased lung function (lower FEV₁), perhaps via similar mechanisms as S1P-induced airway hyperresponsiveness (Roviezzo et al., 2007).

Given these observations of S1P and FTY720, we explored the barrier-regulatory capacity of several novel, synthetic analogues of FTY720. We now demonstrate the similar, but not identical, barrier-regulatory mechanisms of these analogues to S1P and FTY720, with one class of analogues producing significant barrier disruption despite structural similarities. Finally, our *in vivo* data demonstrate that the representative (S)-phosphonate analogue of FTY720 significantly reduces LPS-induced vascular leak in a murine model of inflammatory lung injury. These studies advance our understanding of pulmonary vascular permeability and characterize four novel FTY720 analogues that

JPET #153544

may potentially act as improved therapeutic tools for prevention and reversal of vascular leak.

METHODS

Reagents. S1P was purchased from Sigma (St. Louis, MO), and FTY720 was generously provided by Novartis (Basel, Switzerland). All other reagents were obtained from Sigma, unless otherwise noted. Immunofluorescent and western blotting reagents were obtained as follows: Texas-Red phalloidin (Invitrogen, Carlsbad, CA); rabbit anti-diphosphorylated MLC, rabbit anti-pan MLC, rabbit anti-phosphorylated ERK, rabbit anti-pan ERK (Cell Signaling, Beverly, MA). The labeled dextran vascular permeability assay kit was purchased from Millipore (Bedford, MA). Fura-2AM was obtained through Invitrogen. Pertussis toxin and genestein were purchased from EMD (San Diego, CA).

FTY720 analogue synthesis. Analogues were synthesized as described elsewhere (Lu et al., 2009).

Cell Culture. Human pulmonary artery endothelial cells (HPAEC) were obtained from Lonza (Walkersville, MD) and were cultured as previously described (Dudek et al., 2004) in the manufacturer's recommended Endothelial Growth Medium-2 (EGM-2). Cells were grown at 37°C in a 5% CO₂ incubator, and passages 6-9 were used for experiments. Media was changed one day prior to experimentation.

Transendothelial monolayer electrical resistance. EC were grown to confluency in polycarbonate wells containing evaporated gold microelectrodes, and TER measurements were performed using an electrical cell-substrate impedance sensing

system (ECIS) (Applied Biophysics, Troy, NY) as previously described in detail (Garcia et al., 2001). TER values from each microelectrode were pooled as discrete time points and plotted versus time as the mean \pm SEM.

Vascular permeability assay. A transendothelial permeability assay was performed as we previously described (Garcia et al., 1986) utilizing labeled tracer flux across confluent EC grown on confluent polycarbonate filters (Vascular Permeability Assay Kit, Millipore). Briefly, EC grown to confluency on transwell inserts were exposed to agonist stimulation for 1 hr. After stimulation, FITC-labeled dextran was added to the luminal compartment for 2 hr, and then FITC-dextran clearance across the filter to the abluminal compartment was measured by relative fluorescence excitation at 485 nm and emission at 530 nm.

Immunofluorescence. EC were grown on gelatinized cover slips before exposure to various conditions as described for individual experiments. EC were then fixed in 3.7% formaldehyde for 10 min, permeabilized with 0.25% Triton-X100 for 5 min, washed in PBS, blocked with 2%BSA in TBS-T for 1 hr, and then incubated for 1 hr at room temperature with the primary antibody of interest. After washing, EC were incubated with the appropriate secondary antibody conjugated to immunofluorescent dyes (or Texas-Red conjugated phalloidin for actin staining) for 1 hr at room temperature. After further washing with TBS-T, coverlips were mounted using Prolong™ Anti-Fade Reagent (Invitrogen) and analyzed using a Nikon Eclipse TE2000 inverted microscope.

JPET #153544

Western blotting. After treatment as outlined for individual experiments, EC were subsequently washed with cold Ca^{2+} /Mg-free PBS and lysed with 0.3% SDS lysis buffer containing protease inhibitors (1 mM EDTA, 1 mM PMSF, 1 mM sodium orthovanadate, 1 mM sodium fluoride, 0.2 TIU/ml aprotinin, 10 μM leupeptin, 5 μM pepstatin A). Sample proteins were separated with 4-15% SDS-PAGE gels (Bio-Rad, Hercules, CA) and transferred onto Immobilon-P PVDF membranes (Millipore). Membranes were then immunoblotted with primary antibodies (1:500-1000, 4°C, overnight) followed by secondary antibodies conjugated to HRP (1:5000, room temperature, 30 min) and detected with enhanced chemiluminescence (Pierce ECL or SuperSignal West Dura, Pierce Biotechnology, Rockford, IL) on Biomax MR film (Kodak, Rochester, NY).

Measurement of intracellular calcium. Measurements of $[\text{Ca}^{2+}]_c$ using Fura-2 were performed as previously described (Harbeck et al., 2006). HPAEC plated on 25 mm glass coverslips were loaded with 1 μM Fura-2 acetoxymethyl ester (Molecular Probes, Inc.) for 20 min at 37 °C in KRBH5 buffer (Krebs-Ringer bicarbonate solution containing 119 mM NaCl, 4.7 mM KCl, 2.5 mM CaCl_2 , 1 mM MgCl_2 , 1 mM KH_2PO_4 , 25 mM NaHCO_3 , 10 mM HEPES-NaOH (pH 7.40), and 5 mM glucose). Following replacement of the Fura-2 loading buffer with fresh KRBH5, coverslips were placed into the specimen stage of an inverted fluorescence microscope (Nikon TE-2000U). A Nikon Super Fluor 10X objective was used for these studies. 340- and 380-nm excitation filters and a 530-nm emission filter were used for Fura-2 dual excitation ratio imaging. Imaging data acquisition and analysis were accomplished using MetaMorph/MetaFluor software (Universal Imaging Corp.) and OriginPro 7E (OriginLab Corp.). Fura-2 340/380 dual

excitation ratios were converted to $[Ca^{2+}]$ by *in-situ* calibration. To calibrate Fura-2 ratios, R_{max} was obtained by treating cells with 10 μ M ionomycin and 2.5 mM Ca^{2+} , and R_{min} was obtained by treating cells with EGTA to a final concentration of 10 mM. Fura-2 ratios were converted to $[Ca^{2+}]$ as described by Grynkiewicz *et al* (Grynkiewicz *et al.*, 1985), using the equation:

$$[Ca^{2+}] = K'_d [(R - R_{min}) / (R_{max} - R)] * S_f / S_b$$

Where K'_d is the dissociation constant for Fura-2 in the cytosol (225 nM), and S_f and S_b are the measured emission intensities at 380 nm for Ca^{2+} -free and Ca^{2+} -bound Fura-2, respectively. Data summaries for all Ca^{2+} measurements are expressed as the means \pm S.E.

Animals housing and procedures. All experiments and animal care procedures were approved by the Chicago University Animal Resource Center and were handled according to the Animal Care and Use Committee Guidelines at the University of Chicago. C57BL/6 (20-25 g) mice were purchased from Jackson Laboratory (Bar Harbor, ME). Mice were housed with access to food and water in a temperature-controlled room with a 12 hr dark/light cycle. For experiments performed in the intact animal, male C57BL/6 mice (8–10 weeks) were anesthetized with intraperitoneal ketamine and acetylpromazine mixture according to the approved protocol. *E coli* LPS solution (2.5 mg/kg) or sterile saline was instilled intratracheally via a 20-gauge catheter. Simultaneously, mice received intraperitoneally either FTY720 or analogues

(in doses: 0.01, 0.1, 0.5, 1 and 5 mg/kg) or PBS as vehicle. The animals were allowed to recover for 18 hr. BAL and lungs were collected and stored at -70° C for evaluation of lung injury.

Quantification of total protein and leukocytes analysis in BAL. Collected BAL was centrifuged (1500 g, 15 min 4° C) and, after a second centrifugation of the supernatant (5000 g, 20 min, 4° C), pure BAL fluid was used to measure total protein according to the manufacturer's BCA protein assay kit manual (Bio-Rad). Cell pellets were suspended in Hank's solution and red blood cells were lysed by hypotonic shock (0.2% NaCl) for 5 min. After the cell suspensions were centrifuged and diluted in Hank's solution, an aliquot of the cell suspension was examined for the total number of white blood cells using a hemocytometer. Cytospin slides were prepared from cell suspensions. After Diff-Quik staining, the differential cell count of neutrophils and macrophages was determined by counting 300 cells under a microscope.

Measurement of albumin concentration by ELISA. Pure BAL fluids prepared for protein measurement or MPO lung homogenates were used to test albumin concentration. The assay was performed in 96-well plastic plates (Nalge Nunc A/S, Roskilde, Denmark). Plates were coated with mouse albumin (Bethyl Lab, Montgomery, TX), washed, and blocked. Then, 100- μ l aliquots of the sample or standard and 100 μ l of goat anti-mouse albumin antibody (HRP-conjugated) (1:50,000) were added, followed by incubation at 37°C for 1 hr. Finally, the substrate 3,3',5,5'-tetramethylbenzidine (TMB) was added for

JPET #153544

10 min, and the reaction was stopped by adding 100 μ l of 2 M H₂SO₄. The absorbance at 450 nm was read on a Kinetic microplate reader (Molecular Devices).

Determination of myeloperoxidase activity (MPO). MPO was isolated and measured from snap frozen right lungs as previously described (Remick et al., 1990). The right lung was homogenized in 1 ml of 50 mM potassium phosphate, pH 6.0, with 0.5% hexadecyltrimethylammonium bromide. The resulting homogenate was sonicated and then centrifuged at 12,000 g for 15 min. The supernatant was mixed 1:30 with assay buffer (100 mM potassium phosphate, pH 6.0, 0.005% H₂O₂, 0.168 mg/ml *o*-dianisidine hydrochloride) and the absorbance was read at 490 nm. MPO units were calculated as the change in absorbance with respect to time.

Peripheral blood analysis. The peripheral blood was examined by the Missouri University research animal diagnostic laboratory (Columbia, Missouri) for determination of total blood cell counts and differentials in blood samples.

Statistical analysis. Values are shown as the mean \pm SE. Data were analyzed using a standard Student's *t*-test or one-way ANOVA, groups were compared by Newman-Keuls test, and significance in all cases was defined at $p < 0.05$.

RESULTS

Differential effects of FTY720 analogues on endothelial cell barrier function in vitro.

Novel (R)- and (S)-enantiomers of three FTY720 analogues (**1=phosphonate**, **2=enephosphonate**, and **3=regioisomer**) were synthesized as described (Lu et al., 2009) (see **Figure 1** for the structures of the FTY720 analogues used in this study). Our initial studies examined the effects of these 6 compounds on EC barrier integrity as measured by transendothelial monolayer electrical resistance (TER), a highly sensitive *in vitro* measure of permeability. The (R)- and (S)-enantiomers of 1 and 2 are similar to S1P in that they produce rapid and sustained increases in TER (indicative of enhanced EC barrier function), whereas FTY720 itself induced a delayed onset of barrier enhancement as we have previously reported (Dudek et al., 2007) that was slower to rise in TER relative to S1P and the FTY720 analogues (**Figure 2a**—note that only (R)-enantiomer TER data are shown—(S)-enantiomer results are similar and not shown for simplicity). Interestingly, the FTY720 regioisomers 3R and 3S (in which the positions of the amino and one of the hydroxymethyl groups are interchanged) were barrier disruptive at similar concentrations despite being structurally very similar to the parent FTY720 compound (**Figure 1**), indicating the sensitivity of this response to minor structural alterations. Although similar to S1P in the rapid induction of increased TER, the barrier-enhancing FTY720 analogues 1R, 1S, and 2R have a greater maximal percentage TER change at 1 μ M compared to both S1P and FTY720 (**Figure 2b**). Moreover, when the concentration of these compounds is increased to 10 μ M, analogues 1R, 1S, and 2R exhibit even greater maximal TER elevation, whereas S1P,

FTY720, and 2S are now somewhat barrier disruptive at this dose (**Figure 2c**), indicating that the barrier-enhancing effects of analogues 1R, 1S, and 2R are sustained over a wider concentration range than those of either S1P or FTY720. In fact, dose response titrations of 1S, 1R, and 2R demonstrate that these analogues retain near maximal barrier-promoting effects over a range from 1 μ M to 50 μ M, suggesting a potential broader therapeutic index for these compounds compared to S1P or FTY720 (data not shown). The results also highlight the importance of enantiomer-specific effects as the enephosphonate analogues (2R, 2S) have diametrically opposed effects on EC barrier function at higher concentrations ($\geq 10 \mu$ M).

As a complementary approach to further characterize the barrier-protective effects of these FTY720 analogues *in vitro*, we next assayed permeability of FITC-labeled dextran across the pulmonary EC monolayer (Garcia et al., 1986). While TER measurements are an assessment of EC permeability in terms of resistance to an electrical current, this assay allows for characterization of changes in EC permeability to higher molecular weight molecules. Compared to control EC, those treated with S1P, FTY720, or FTY720 analogues 1 and 2 all demonstrate significantly decreased permeability in this assay consistent with the TER data shown above (**Figure 3**). In contrast, the regioisomers (3R, 3S) increase EC permeability to a degree similar to thrombin, a well-described and potent barrier-disrupting agent (Dudek and Garcia, 2001).

Differential cytoskeletal rearrangement and intracellular signaling of FTY720 analogues.

S1P generates dramatic EC cytoskeletal rearrangements such as enhanced cortical actin accumulation and peripheral MLC phosphorylation (Garcia et al., 2001) which are not observed during FTY720-induced barrier enhancement (Dudek et al., 2007). Since the barrier enhancing analogues 1 and 2 produce immediate TER elevation similar to S1P (**Figure 2a**), we next evaluated whether these compounds elicited rapid F-actin cytoskeletal rearrangements similar to exposure to S1P (**Figure 4a**). Immunofluorescent analysis reveals that compounds 1 and 2 rapidly induce (within 5 min) increased cortical actin ring formation in the periphery of pulmonary EC characteristic of S1P-induced barrier enhancement (arrows, **Figure 4a**) (Garcia et al., 2001). In contrast, as we have reported previously (Dudek et al., 2007), FTY720 fails to elicit cortical actin ring formation early at 5 min (data not shown) or at data time points (30 min) associated with peak TER elevation (**Figure 2a**). Interestingly, the barrier-disrupting FTY720 analogue 3 does not produce dramatic F-actin rearrangements.

Whereas the barrier-enhancing FTY analogues exhibit similarities to S1P in cortical actin ring formation, their effects on intracellular signaling events are varied (**Figure 4b**). Evaluation of EC lysates for MLC and ERK phosphorylation demonstrate increased MLC and ERK phosphorylation at 5 min in response to S1P, while analogues 1R and 2R cause increased phosphorylation of ERK at 5 min. Neither FTY720 nor any of its analogues induce significant MLC phosphorylation over this time frame. Interestingly, the enantiomers 1S and 2S differ from 1R and 2R in terms of ERK signaling as the former fail to induce phosphorylation of this kinase. Thus, these closely related compounds are not equivalent in terms of their downstream signaling effects on cultured pulmonary EC. The barrier disruptive FTY regioisomers 3R and 3S do not

increase ERK or MLC phosphorylation (5 min), unlike the well-described barrier-disruptive agent thrombin (Dudek and Garcia, 2001).

To further explore the mechanistic differences in barrier regulation, intracellular calcium responses to the FTY720 analogues, S1P, and FTY720 were examined. Previous studies have described a brief but substantial increase in intracellular calcium (Ca^{2+}) following S1P exposure in pulmonary endothelial cells (Garcia et al., 2001), whereas FTY720 fails to increase intracellular Ca^{2+} (Dudek et al., 2007). Changes in HPAEC $[\text{Ca}^{2+}]_i$ after treatment with FTY720 analogues, S1P, FTY720, and vehicle (all at 1 μM concentration) revealed that only S1P produced a transient Ca^{2+} spike (**Figure 5**), demonstrating that the FTY720 analogue-induced barrier enhancement does not require the calcium signaling observed in association with S1P.

Mechanistic components of FTY720 analogue induced barrier enhancement.

We next pursued a series of experiments designed to mechanistically explore the manner in which these FTY720 analogues produce barrier enhancement. Similar to S1P and FTY720 (Dudek et al., 2007), TER elevation induced by all four barrier-enhancing compounds (1R, 1S, 2R, 2S) is significantly inhibited by preincubation with either pertussis toxin (PTX) or genistein, a nonspecific tyrosine kinase inhibitor (**Table 1**), indicating essential involvement of G_i -coupled signaling and tyrosine phosphorylation events in these barrier-enhancing responses. We have also previously reported that signaling pathways initiated in membrane lipid rafts are essential to S1P- and FTY720-induced barrier enhancement (Singleton et al., 2005; Dudek et al., 2007). Consistent with the involvement of lipid rafts in FTY720 analogue barrier enhancement, the lipid raft

disrupting agent, methyl- β -cyclodextrin (M β CD), significantly attenuates their TER elevation (**Table 1**). Overall, these *in vitro* data support a barrier enhancing pathway induced by FTY720 analogues 1R, 1S, 2R, 2S that likely includes lipid raft signaling and G_i-linked receptor coupling to downstream tyrosine phosphorylation events.

FTY720 analogue 1S is protective in a LPS-induced murine lung injury model.

To extend our *in vitro* findings that the FTY720 analogues promote lung EC integrity, we employed a well characterized murine model of LPS-induced lung injury (see Methods) to examine the *in vivo* effects of these compounds on pulmonary vascular leak and inflammatory injury. Preliminary studies indicated that 1S was superior to the other barrier-promoting analogues (1R, 2R, 2S) in this model (data not shown). Therefore, we proceeded to further characterize the representative barrier-enhancing FTY720 analogue 1S on pulmonary vascular leak and inflammatory injury in this mouse model. As we have previously described (Peng et al., 2004), intratracheal administration of LPS (2.5 mg/kg) produces significant murine inflammatory lung injury at 18 hr as assessed by measurements of BAL total protein and cell count, BAL albumin, and lung tissue albumin. Moreover, LPS increases tissue MPO activity, another reflection of lung parenchymal phagocyte infiltration, compared with control mice (Peng et al., 2004). Intraperitoneal injection of a single dose of FTY720 analogue 1S (0.1-5.0 mg/kg) delivered 1 hr after LPS exposure significantly reduces capillary leak relative to PBS control at all concentrations studied as measured by total BAL protein concentrations (**Figure 6a**). This reduction in permeability by 1S is comparable to that achieved by S1P or FTY720. In addition, 1S significantly reduces LPS-induced

albumin leakage from the vascular space into both the surrounding lung tissue and BAL (**Figure 6b-c**), as well as BAL WBC accumulation and lung tissue MPO activity (**Figure 7a-b**). These combined data suggest that the optimal protective dose of 1S is 0.1-1.0 mg/kg in this model.

One potential concern when using FTY720 or related compounds in sepsis-related processes such as acute lung injury is the known lymphopenia effect of the parent compound (Kovarik et al., 2004). Therefore, peripheral blood WBC levels were assessed in this mouse model. For comparison, at baseline in control mice (no LPS), total circulating WBC is $4.11 \pm 1.58 \times 10^3/\mu\text{l}$, and the lymphocyte count is $3.57 \pm 1.74 \times 10^3/\mu\text{l}$ ($n = 6$), so these levels are significantly suppressed ($p \leq .001$ for both total WBC and lymphocyte count) by LPS alone in this model 18 hr after its administration (**Figure 8**). However, 1S treatment in these mice does not further alter peripheral blood leukocyte and lymphocyte levels relative to PBS controls (**Figure 8**), suggesting that the 1S analogue does not produce additional immunosuppression in this LPS model. Interestingly, FTY720 itself also does not suppress circulating WBC levels relative to PBS controls in this model of inflammatory lung injury. In summary, the FTY720 analogue 1S decreases multiple indices of LPS-induced pulmonary injury in this murine model without apparent hematologic toxicity.

DISCUSSION

In this study, we demonstrate potent pulmonary vascular permeability effects of several novel FTY720 analogues both *in vitro* and *in vivo*. These findings have direct therapeutic relevance for the Acute Lung Injury/Acute Respiratory Distress Syndrome (ALI/ARDS), a highly morbid condition afflicting an estimated 200,000 people annually and causing 75,000 deaths in the United States (Rubenfeld et al., 2005). To date, there are no effective interventions that target the critical pulmonary vascular leak that underlies this syndrome (Wheeler and Bernard, 2007). Our laboratory group was the first to identify the potential of S1P to serve in a vascular barrier-enhancing capacity *in vitro* (Garcia et al., 2001); however, our more recent animal work suggests that modulation of S1P-related pathways in lung endothelium also holds promise *in vivo* with S1P infusion into murine and canine models of inflammatory lung injury highly protective (McVerry et al., 2004; Peng et al., 2004), while others have demonstrated that administration of an S1P₁R antagonist induces lung capillary leakage (Sanna et al., 2006). Unfortunately, the endogenous compound S1P is a suboptimal therapeutic candidate because of its potential to produce negative effects, including cardiac toxicity and pulmonary edema at higher doses (Forrest et al., 2004; Gon et al., 2005). In fact, multiple agents for inhibiting various components of the S1P pathway are currently under therapeutic investigation for various clinical indications (Takabe et al., 2008). Since the structurally related synthetic compound FTY720 exhibits potent barrier-enhancing properties both *in vitro* and *in vivo* (Sanchez et al., 2003; Peng et al., 2004; Dudek et al., 2007) and is in advanced clinical trials for treatment of multiple sclerosis

(Brown et al., 2007), it remains a promising alternative to S1P that may soon be available for trials in patients with ALI. However, FTY720 has demonstrated bradycardic and immunosuppressive effects (Kovarik et al., 2004; Brown et al., 2007; Tedesco-Silva et al., 2007) that may be detrimental to critically ill patients with ALI.

Therefore, we generated multiple analogues of FTY720 to further our mechanistic understanding of how these compounds regulate EC barrier regulation in the hopes of designing a more optimal therapeutic agent. Other groups have synthesized multiple derivatives of FTY720, including phosphonates (Mandala et al., 2002; Forrest et al., 2004; Hale et al., 2004b), phosphothioates (Foss et al., 2005), 4(5)-phenylimidazole-containing (Clemens et al., 2005), and conformationally constrained analogues (Hanessian et al., 2007; Zhu et al., 2007), primarily for the purposes of characterizing them in terms of S1P receptor affinity and the ability to induce lymphopenia. Additional analogues have been employed to evaluate the pro-apoptotic effects of sphingosine and FTY720 (Don et al., 2007), or as possible anti-angiogenic agents (Nakayama et al., 2008). However, this report is the first to use this valuable pharmacological approach to explore the potential of FTY720-related compounds to regulate pulmonary vascular permeability.

Our data illustrate the usefulness of this approach as the FTY720 analogues described here exhibit dramatically differential effects on lung EC barrier function. The FTY720 phosphonate (1R, 1S) and enephosphonate (2R, 2S) compounds display *in vitro* barrier enhancing properties comparable or superior to S1P and FTY720, while the FTY720 regioisomers (3R, 3S) are barrier disruptive despite being structurally very similar to the parent FTY720 compound (**Figures 2b, 3**). These results suggest that

three of the barrier-enhancing analogues (1R, 1S, 2R) may be more appealing as potential clinical agents than S1P or FTY720 for blocking ALI-associated pulmonary edema as they exhibit a broader therapeutic index with increased potency *in vitro* (**Figure 2b,c**). Our preliminary mechanistic studies indicate that G_i-coupled receptor signaling, tyrosine kinases, and lipid raft domains are involved in mediating the enhanced EC barrier function induced by these analogues, as they are in the S1P response (**Table 1**). Ongoing studies are seeking to determine the signaling events that account for the differential effects of these compounds on EC barrier function. One intriguing possibility is that FTY720 phosphonate and enephosphonate compounds may not be hydrolyzed by lipid phosphatases since a similar mechanism was noted to result in differential intracellular signaling for a S1P phosphonate analogue (Zhao et al., 2007).

Our data further demonstrate that orientation changes present in the regioisomers compared to FTY720 are sufficient to produce opposite effects on EC permeability. Understanding how these effects are mediated may provide important additional insights into EC barrier regulation. The mechanism through which 3R and 3S disrupt the EC barrier does not appear to involve MLC phosphorylation, actin stress fiber formation, or actomyosin contraction (**Figure 4**) as observed after thrombin (Dudek and Garcia, 2001). Our data also highlight the importance of stereoisomeric structure in determining the bioactivity of these compounds in barrier regulation. Although FTY720 phosphonate (compound 1 in this study) has been synthesized previously by others (Mandala et al., 2002; Forrest et al., 2004; Hale et al., 2004b), these prior studies used only a racemic mixture that did not differentiate enantiomeric-specific effects. Such effects are known to be functionally important in the metabolism of the parent

compound, FTY720, as measurements in rats and humans demonstrate that *in vivo* phosphorylation of FTY720 results only in formation of the (S)-enantiomer of FTY-phosphate, which is a much higher affinity agonist for the S1P receptor family than (R)-FTY-phosphate (Albert et al., 2005). In the present study, several interesting properties differentiate the (R)- and (S)-enantiomers of FTY720 phosphonate and enephosphonate. For example, 1R and 2R rapidly activate ERK while the (S)-enantiomers of these compounds do not (**Figure 4b**). Although 10 μ M of 2R potently increases EC barrier function *in vitro*, this concentration of 2S is barrier disruptive (**Figure 2c**). Finally, the 1S phosphonate compound is more efficacious than 1R in the mouse model of LPS-induced lung injury (data not shown). Thus, further study of the chiral effects of these compounds on EC barrier function is warranted.

An important aspect of mechanistically characterizing these analogues is to determine their relative S1P receptor activities. Most relevant are their effects on S1P₁R and S1P₃R since these are the best described S1P receptors in terms of their respective barrier-enhancing (S1P₁R) (Garcia et al., 2001; Singleton et al., 2005; Sanna et al., 2006) and barrier-disrupting (S1P₃R) (Gon et al., 2005) properties. Recently published data characterizes the relative activity of the four barrier-enhancing analogues (1S, 2S, 1R, 2R) on S1P₁R (Lu et al., 2009). In this study, HTC4 cells (which do not express endogenous S1P receptors) were stably transfected with S1P₁R, and Ca²⁺ mobilization assays performed after stimulation with various concentrations of S1P, FTY720-phosphate, and analogues. The 1R (93% of maximal S1P response) and the 2R (73%) analogues exhibited substantial S1P₁R activation in these assays similar to that of FTY720-P (76%) (Lu et al., 2009) and consistent with this receptor being the

primary transducer of barrier enhancement by these analogues. In contrast, 1S produced only 36% of the maximal S1P response despite exhibiting comparable barrier-enhancing potency to the other compounds (**Figs. 2, 3**). These interesting data suggest that barrier enhancement by 1S may be transduced at least in part via another receptor as we have previously suggested for FTY720 itself (Dudek et al., 2007). Another intriguing possibility is that the 1S analogue may alter the conformational state of S1P₁R leading to differential effector coupling and altered downstream signaling that results in reduced Ca²⁺ mobilization but comparable barrier enhancement. A similar model of S1P₁R signaling involving multiple conformational states has been proposed by others (Pyne and Pyne, 2008). Even more robust evidence for an alternative barrier-enhancing receptor is provided by 2S, which is capable of significantly improving EC barrier function (**Figs. 2, 3**) despite a complete inability to activate the S1P₁R as measured by this Ca²⁺ mobilization assay (Lu et al., 2009).

In addition, this same group has characterized the relative activity of 1S, 2S, 1R, and 2R on S1P₃R in the Ca²⁺ mobilization assay (W.J. Valentine and G. Tigyi, personal communication). Importantly, these barrier-enhancing analogues all exhibit little (1R, 2R ~10% of maximal S1P response) or no (1S, 2S both 0%) S1P₃R activity as measured by Ca²⁺ mobilization. Thus, all of the barrier-enhancing analogues identified in our study may have therapeutic advantages over S1P and FTY720 in terms of decreasing the S1P₃R-related negative effects on barrier function and cardiac toxicity (Forrest et al., 2004; Hale et al., 2004a; Gon et al., 2005). The S1P receptor profiles of the barrier-disrupting FTY720 analogues identified in our study (3S, 3R) also merit further study.

In summary, these results provide important mechanistic insights into the regulation of EC barrier function and demonstrate the potential therapeutic utility of several novel FTY720 analogues to reverse the pulmonary vascular leak that characterizes ALI. (S)-FTY720-phosphonate is particularly promising both *in vitro* and *in vivo*. Moreover, animal data presented here suggest that at doses sufficient to protect against lung injury, FTY720 and its derivative 1S do not adversely affect circulating WBC levels during inflammatory states (**Figure 8**), and thus may be appropriate to use in critically ill patients with infection-associated ALI. Given the high mortality of this syndrome and lack of specific therapies (Wheeler and Bernard, 2007), clinical trials of these agents in ALI may be warranted in the near future.

REFERENCES

- Albert R, Hinterding K, Brinkmann V, Guerini D, Muller-Hartweg C, Knecht H, Simeon C, Streiff M, Wagner T, Welzenbach K, Zecri F, Zollinger M, Cooke N and Francotte E (2005) Novel immunomodulator FTY720 is phosphorylated in rats and humans to form a single stereoisomer. Identification, chemical proof, and biological characterization of the biologically active species and its enantiomer. *J Med Chem* **48**:5373-5377.
- Brinkmann V, Cyster JG and Hla T (2004) FTY720: sphingosine 1-phosphate receptor-1 in the control of lymphocyte egress and endothelial barrier function. *Am J Transplant* **4**:1019-1025.
- Brown BA, Kantesaria PP and McDevitt LM (2007) Fingolimod: a novel immunosuppressant for multiple sclerosis. *Ann Pharmacother* **41**:1660-1668.
- Clemens JJ, Davis MD, Lynch KR and Macdonald TL (2005) Synthesis of 4(5)-phenylimidazole-based analogues of sphingosine-1-phosphate and FTY720: discovery of potent S1P1 receptor agonists. *Bioorg Med Chem Lett* **15**:3568-3572.
- Don AS, Martinez-Lamenca C, Webb WR, Proia RL, Roberts E and Rosen H (2007) Essential requirement for sphingosine kinase 2 in a sphingolipid apoptosis pathway activated by FTY720 analogues. *J Biol Chem* **282**:15833-15842.
- Dudek SM, Camp SM, Chiang ET, Singleton PA, Usatyuk PV, Zhao Y, Natarajan V and Garcia JG (2007) Pulmonary endothelial cell barrier enhancement by FTY720 does not require the S1P1 receptor. *Cell Signal* **19**:1754-1764.

- Dudek SM and Garcia JG (2001) Cytoskeletal regulation of pulmonary vascular permeability. *J Appl Physiol* **91**:1487-1500.
- Dudek SM, Jacobson JR, Chiang ET, Birukov KG, Wang P, Zhan X and Garcia JG (2004) Pulmonary endothelial cell barrier enhancement by sphingosine 1-phosphate: roles for cortactin and myosin light chain kinase. *J Biol Chem* **279**:24692-24700.
- Forrest M, Sun SY, Hajdu R, Bergstrom J, Card D, Doherty G, Hale J, Keohane C, Meyers C, Milligan J, Mills S, Nomura N, Rosen H, Rosenbach M, Shei GJ, Singer, II, Tian M, West S, White V, Xie J, Proia RL and Mandala S (2004) Immune cell regulation and cardiovascular effects of sphingosine 1-phosphate receptor agonists in rodents are mediated via distinct receptor subtypes. *J Pharmacol Exp Ther* **309**:758-768.
- Foss FW, Jr., Clemens JJ, Davis MD, Snyder AH, Zigler MA, Lynch KR and Macdonald TL (2005) Synthesis, stability, and implications of phosphothioate agonists of sphingosine-1-phosphate receptors. *Bioorg Med Chem Lett* **15**:4470-4474.
- Garcia JG, Liu F, Verin AD, Birukova A, Dechert MA, Gerthoffer WT, Bamburg JR and English D (2001) Sphingosine 1-phosphate promotes endothelial cell barrier integrity by Edg-dependent cytoskeletal rearrangement. *J Clin Invest* **108**:689-701.
- Garcia JG, Siflinger-Birnboim A, Bizios R, Del Vecchio PJ, Fenton JW, 2nd and Malik AB (1986) Thrombin-induced increase in albumin permeability across the endothelium. *J Cell Physiol* **128**:96-104.

- Gon Y, Wood MR, Kiosses WB, Jo E, Sanna MG, Chun J and Rosen H (2005) S1P3 receptor-induced reorganization of epithelial tight junctions compromises lung barrier integrity and is potentiated by TNF. *Proc Natl Acad Sci U S A* **102**:9270-9275.
- Grynkiewicz G, Poenie M and Tsien RY (1985) A new generation of Ca²⁺ indicators with greatly improved fluorescence properties. *J Biol Chem* **260**:3440-3450.
- Hale JJ, Doherty G, Toth L, Mills SG, Hajdu R, Keohane CA, Rosenbach M, Milligan J, Shei GJ, Chrebet G, Bergstrom J, Card D, Forrest M, Sun SY, West S, Xie H, Nomura N, Rosen H and Mandala S (2004a) Selecting against S1P3 enhances the acute cardiovascular tolerability of 3-(N-benzyl)aminopropylphosphonic acid S1P receptor agonists. *Bioorg Med Chem Lett* **14**:3501-3505.
- Hale JJ, Neway W, Mills SG, Hajdu R, Ann Keohane C, Rosenbach M, Milligan J, Shei GJ, Chrebet G, Bergstrom J, Card D, Koo GC, Koprak SL, Jackson JJ, Rosen H and Mandala S (2004b) Potent S1P receptor agonists replicate the pharmacologic actions of the novel immune modulator FTY720. *Bioorg Med Chem Lett* **14**:3351-3355.
- Hanessian S, Charron G, Billich A and Guerini D (2007) Constrained azacyclic analogues of the immunomodulatory agent FTY720 as molecular probes for sphingosine 1-phosphate receptors. *Bioorg Med Chem Lett* **17**:491-494.
- Harbeck MC, Chepurny O, Nikolaev VO, Lohse MJ, Holz GG and Roe MW (2006) Simultaneous optical measurements of cytosolic Ca²⁺ and cAMP in single cells. *Sci STKE* **2006**:pl6.

- Kappos L, Antel J, Comi G, Montalban X, O'Connor P, Polman CH, Haas T, Korn AA, Karlsson G and Radue EW (2006) Oral fingolimod (FTY720) for relapsing multiple sclerosis. *N Engl J Med* **355**:1124-1140.
- Kovarik JM, Schmouder RL and Slade AJ (2004) Overview of FTY720 clinical pharmacokinetics and pharmacology. *Ther Drug Monit* **26**:585-587.
- Lu X, Sun C, Valentine WJ, Shuyu E, Liu J, Tigyi G and Bittman R (2009) Chiral vinylphosphonate and phosphonate analogues of the immunosuppressive agent FTY720. *J Org Chem* **74**:3192-3195.
- Mandala S, Hajdu R, Bergstrom J, Quackenbush E, Xie J, Milligan J, Thornton R, Shei GJ, Card D, Keohane C, Rosenbach M, Hale J, Lynch CL, Rupprecht K, Parsons W and Rosen H (2002) Alteration of lymphocyte trafficking by sphingosine-1-phosphate receptor agonists. *Science* **296**:346-349.
- Mansoor M and Melendez AJ (2008) Recent trials for FTY720 (fingolimod): a new generation of immunomodulators structurally similar to sphingosine. *Rev Recent Clin Trials* **3**:62-69.
- Matloubian M, Lo CG, Cinamon G, Lesneski MJ, Xu Y, Brinkmann V, Allende ML, Proia RL and Cyster JG (2004) Lymphocyte egress from thymus and peripheral lymphoid organs is dependent on S1P receptor 1. *Nature* **427**:355-360.
- McVerry BJ, Peng X, Hassoun PM, Sammani S, Simon BA and Garcia JG (2004) Sphingosine 1-phosphate reduces vascular leak in murine and canine models of acute lung injury. *Am J Respir Crit Care Med* **170**:987-993.
- Nakayama S, Uto Y, Tanimoto K, Okuno Y, Sasaki Y, Nagasawa H, Nakata E, Arai K, Momose K, Fujita T, Hashimoto T, Okamoto Y, Asakawa Y, Goto S and Hori H

- (2008) TX-2152: a conformationally rigid and electron-rich diyne analogue of FTY720 with in vivo antiangiogenic activity. *Bioorg Med Chem* **16**:7705-7714.
- Neviani P, Santhanam R, Oaks JJ, Eiring AM, Notari M, Blaser BW, Liu S, Trotta R, Muthusamy N, Gambacorti-Passerini C, Druker BJ, Cortes J, Marcucci G, Chen CS, Verrills NM, Roy DC, Caligiuri MA, Bloomfield CD, Byrd JC and Perrotti D (2007) FTY720, a new alternative for treating blast crisis chronic myelogenous leukemia and Philadelphia chromosome-positive acute lymphocytic leukemia. *J Clin Invest* **117**:2408-2421.
- Peng X, Hassoun PM, Sammani S, McVerry BJ, Burne MJ, Rabb H, Pearse D, Tuder RM and Garcia JG (2004) Protective effects of sphingosine 1-phosphate in murine endotoxin-induced inflammatory lung injury. *Am J Respir Crit Care Med* **169**:1245-1251.
- Pyne NJ and Pyne S (2008) Sphingosine 1-phosphate, lysophosphatidic acid and growth factor signaling and termination. *Biochim Biophys Acta* **1781**:467-476.
- Remick DG, Strieter RM, Eskandari MK, Nguyen DT, Genord MA, Raiford CL and Kunkel SL (1990) Role of tumor necrosis factor-alpha in lipopolysaccharide-induced pathologic alterations. *Am J Pathol* **136**:49-60.
- Roviezzo F, Di Lorenzo A, Bucci M, Brancaleone V, Vellecco V, De Nardo M, Orlotti D, De Palma R, Rossi F, D'Agostino B and Cirino G (2007) Sphingosine-1-phosphate/sphingosine kinase pathway is involved in mouse airway hyperresponsiveness. *Am J Respir Cell Mol Biol* **36**:757-762.

- Rubinfeld GD, Caldwell E, Peabody E, Weaver J, Martin DP, Neff M, Stern EJ and Hudson LD (2005) Incidence and outcomes of acute lung injury. *N Engl J Med* **353**:1685-1693.
- Sanchez T, Estrada-Hernandez T, Paik JH, Wu MT, Venkataraman K, Brinkmann V, Claffey K and Hla T (2003) Phosphorylation and action of the immunomodulator FTY720 inhibits vascular endothelial cell growth factor-induced vascular permeability. *J Biol Chem* **278**:47281-47290.
- Sanna MG, Wang SK, Gonzalez-Cabrera PJ, Don A, Marsolais D, Matheu MP, Wei SH, Parker I, Jo E, Cheng WC, Cahalan MD, Wong CH and Rosen H (2006) Enhancement of capillary leakage and restoration of lymphocyte egress by a chiral S1P1 antagonist in vivo. *Nat Chem Biol* **2**:434-441.
- Shikata Y, Birukov KG and Garcia JG (2003) S1P induces FA remodeling in human pulmonary endothelial cells: role of Rac, GIT1, FAK and paxillin. *J Appl Physiol* **94**:1193-1203.
- Singleton PA, Dudek SM, Chiang ET and Garcia JG (2005) Regulation of sphingosine 1-phosphate-induced endothelial cytoskeletal rearrangement and barrier enhancement by S1P1 receptor, PI3 kinase, Tiam1/Rac1, and alpha-actinin. *Faseb J* **19**:1646-1656.
- Takabe K, Paugh SW, Milstien S and Spiegel S (2008) "Inside-out" signaling of sphingosine-1-phosphate: therapeutic targets. *Pharmacol Rev* **60**:181-195.
- Tedesco-Silva H, Szakaly P, Shoker A, Sommerer C, Yoshimura N, Schena FP, Cremer M, Hmissi A, Mayer H and Lang P (2007) FTY720 versus mycophenolate mofetil

in de novo renal transplantation: six-month results of a double-blind study.

Transplantation **84**:885-892.

Wheeler AP and Bernard GR (2007) Acute lung injury and the acute respiratory distress syndrome: a clinical review. *Lancet* **369**:1553-1564.

Zhao Y, Kalari SK, Usatyuk PV, Gorshkova I, He D, Watkins T, Brindley DN, Sun C, Bittman R, Garcia JG, Berdyshev EV and Natarajan V (2007) Intracellular generation of sphingosine 1-phosphate in human lung endothelial cells: role of lipid phosphate phosphatase-1 and sphingosine kinase 1. *J Biol Chem* **282**:14165-14177.

Zhu R, Snyder AH, Kharel Y, Schaffter L, Sun Q, Kennedy PC, Lynch KR and Macdonald TL (2007) Asymmetric synthesis of conformationally constrained fingolimod analogues--discovery of an orally active sphingosine 1-phosphate receptor type-1 agonist and receptor type-3 antagonist. *J Med Chem* **50**:6428-6435.

FOOTNOTES

This work was supported by grants from the National Institutes of Health (NIH) National Heart Lung Blood Institute (NHLBI) [grant P01 HL 58064 and R01 68071 (JGNG), R01 HL 79396 (VN), R01 HL 88144 (SMD)], and NIH National Institute of Diabetes and Digestive and Kidney Diseases (NIDDK) [R01 DK074966-02 (MR)].

Reprint requests should be addressed to the corresponding author listed above.

LEGENDS FOR FIGURES

Figure 1. Structures of FTY720 analogues. Enantiomers of FTY720 analogues include: A) (R)-FTY720 Phosphonate, abbreviated 1R; B) (R)-FTY720 Enephosphonate, abbreviated 2R; C) (R)-FTY720 Regioisomer, abbreviated 3R; D) (S)-FTY720 Phosphonate, abbreviated 1S; E) (S)-FTY720 Enephosphonate, abbreviated 2S; and F) (S)-FTY720 Regioisomer, abbreviated 3S.

Figure 2. FTY720 analogues promote TER barrier enhancement. A) HPAEC plated on gold electrodes were stimulated with 1 μ M of S1P (black line), FTY720 (red), 1R (blue), 2R (green), or 3R (purple) at time = 0. The TER tracing represents pooled data (\pm S.E.M.) from four independent experiments. Bar graphs depict pooled TER data from HPAEC stimulated at 1 μ M (B) or 10 μ M (C) with S1P, FTY720, 1R, 1S, 2R, 2S, 3R, or 3S as indicated. The data are expressed as maximal percent TER change (\pm S.E.M.) obtained within 60 min. Positive values indicate barrier enhancement. Negative values indicate barrier disruption. n = 3-5 independent experiments per condition, *p<0.01 vs. other conditions.

Figure 3. FTY720 analogues reduce transwell endothelial cell permeability. A) HPAEC plated on transwell inserts were stimulated with S1P, FTY720, 1R, 1S, 2R, 2S (each at 1 μ M), thrombin (1 unit/ml), 3R, or 3S (both 25 μ M; lower concentrations did not alter permeability) for 1 hr prior to addition of FITC-dextran. After 2 hr incubation, FITC-dextran clearance relative fluorescence was measured by excitation at 485 nm

and emission at 530 nm. Data were normalized to unstimulated control. n = 3 independent experiments per condition, *p<0.01 vs. unstimulated condition.

Figure 4. FTY720 analogues induce cytoskeletal rearrangement. A) Confluent HPAEC were stimulated with vehicle control or 1 μ M S1P, 1R, 2R, or 3R for 5 min, or FTY720 (1 μ M) for 30 min. Cells were fixed using formaldehyde and stained with Texas-Red phalloidin for F-actin. Arrows indicate increased cortical actin. B) Confluent HPAEC were stimulated with S1P, FTY720, and FTY720 analogues at 1 μ M for 5 min, and then lysed for western blotting with phospho-MLC, pan-MLC, phospho-ERK, or pan-ERK antibodies as indicated. Note that all wells represent equal loading of total proteins. Experiments were independently performed in triplicate with representative blots shown.

Figure 5. FTY720 analogues do not stimulate intracellular calcium release. Cultured HPAEC were stimulated with methanol vehicle or 1 μ M S1P, FTY720, 1R, 2R, or 3R at Time 0, and intracellular calcium levels were measured as fold change in $[Ca^{2+}]$ relative to 60 sec average prior to treatment, as determined by Fura-2 as described in Methods. n = 3 independent experiments per condition.

Figure 6. FTY720 analogue 1S reduces LPS-induced vascular permeability in murine lungs. A) Male C57BL/6 mice were given LPS (2.5 mg/kg) intratracheally. One hr later, mice received PBS vehicle, FTY720 (0.5 mg/kg), or 1S (doses labeled on the graph, mg/kg) intraperitoneally, or S1P (0.026 mg/kg) via jugular vein injection

simultaneous with LPS. The treated mice were allowed to recover for 18 hr. BAL fluid was processed to determinate total protein concentrations. $n = 3-5$ animals per condition. $*p < 0.05$ and $**p < 0.01$ compared to PBS vehicle treatment. B) BAL albumin levels were also measured in these animals. $***p < 0.001$ and $**p < 0.01$ compared to PBS vehicle treatment. C) In similarly treated mice, lung tissue albumin was measured. $n = 4-5$ animals per condition. $*p < 0.05$ and $**p < 0.01$ compared to PBS vehicle treatment.

Figure 7. 1S reduces LPS-induced WBC accumulation in mouse lungs. A) In mice treated as described in Fig. 6, BAL fluid was also analyzed for total WBC count. $n = 3-5$ animals per condition. $*p < 0.05$, $**p < 0.01$, and $***p < 0.001$ compared to PBS vehicle treatment. B) In similarly treated mice, lung tissue MPO activity was assayed. $n = 4-6$ animals per condition. $**p < 0.01$ and $***p < 0.001$ compared to PBS vehicle treatment.

Figure 8. Peripheral blood leukocyte counts in FTY720 analogue- and LPS-treated mice. Mice received intratracheal LPS followed one hr later by PBS, FTY720 (0.5 mg/ml), or 1S (doses labeled on the graph, mg/kg) intraperitoneally as described. Blood was collected 18 hr after LPS for total WBC (A) and lymphocytes (B) quantification. $n = 3-7$ animals per condition. There are no statistical differences among any of the conditions shown.

TABLE

% Inhibition of Maximal TER Response (of agonist-only control)			
	PTX**	Gen*	M β CD**
S1P	98.35 (\pm 0.25)	42.4 (\pm 13.9)	81.5 (\pm 8.0)
FTY	84.0 (\pm 9.1)	86.2 (\pm 10.7)	88.1 (\pm 5.6)
1R	79.2 (\pm 5.9)	54.3 (\pm 14.7)	67.0 (\pm 19.7)
1S	92.8 (\pm 2.6)	51.9 (\pm 21.0)	97.2 (\pm 0.8)
2R	88.1 (\pm 7.8)	41.1 (\pm 12.2)	87.4 (\pm 5.4)
2S	76.3 (\pm 12.0)	91.6 (\pm 2.4)	95.2 (\pm 1.0)

Table 1. Pharmacologic inhibitor effects on FTY720 analogue barrier enhancement. Confluent HPAEC were plated on gold microelectrodes and then stimulated with 1 μ M S1P, FTY720, 1R, 1S, 2R, or 2S after either a 2 hr preincubation with 100 ng/ml pertussis toxin (PTX), 30 min preincubation with 200 μ M genistein (Gen), or 2 hr preincubation with 2 mM M β CD (Panel C), or their respective vehicle controls. Data were pooled from multiple TER experiments (4-10 independent experiments per condition) and expressed as percent inhibition of maximal barrier enhancement at 60

JPET #153544

min relative to agonist-only control. **All EC treated with this inhibitor exhibit $p < 0.01$ decreased TER compared with agonist-only control. *All EC treated with this inhibitor exhibit $p < 0.05$ decreased TER compared with agonist-only control.

Figure 1

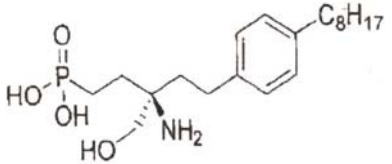
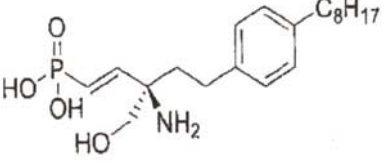
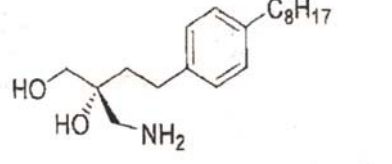
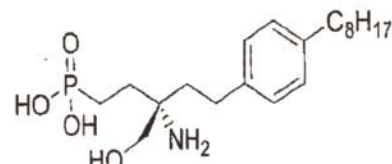
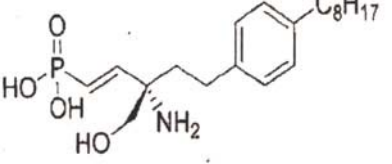
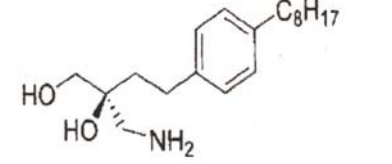
Enantiomer	FTY720 Phosphonate	FTY720 Enephosphonate	FTY720 Regioisomer
(R)	<p>A. (1R)</p> 	<p>B. (2R)</p> 	<p>C. (3R)</p> 
(S)	<p>D. (1S)</p> 	<p>E. (2S)</p> 	<p>F. (3S)</p> 

Figure 2a

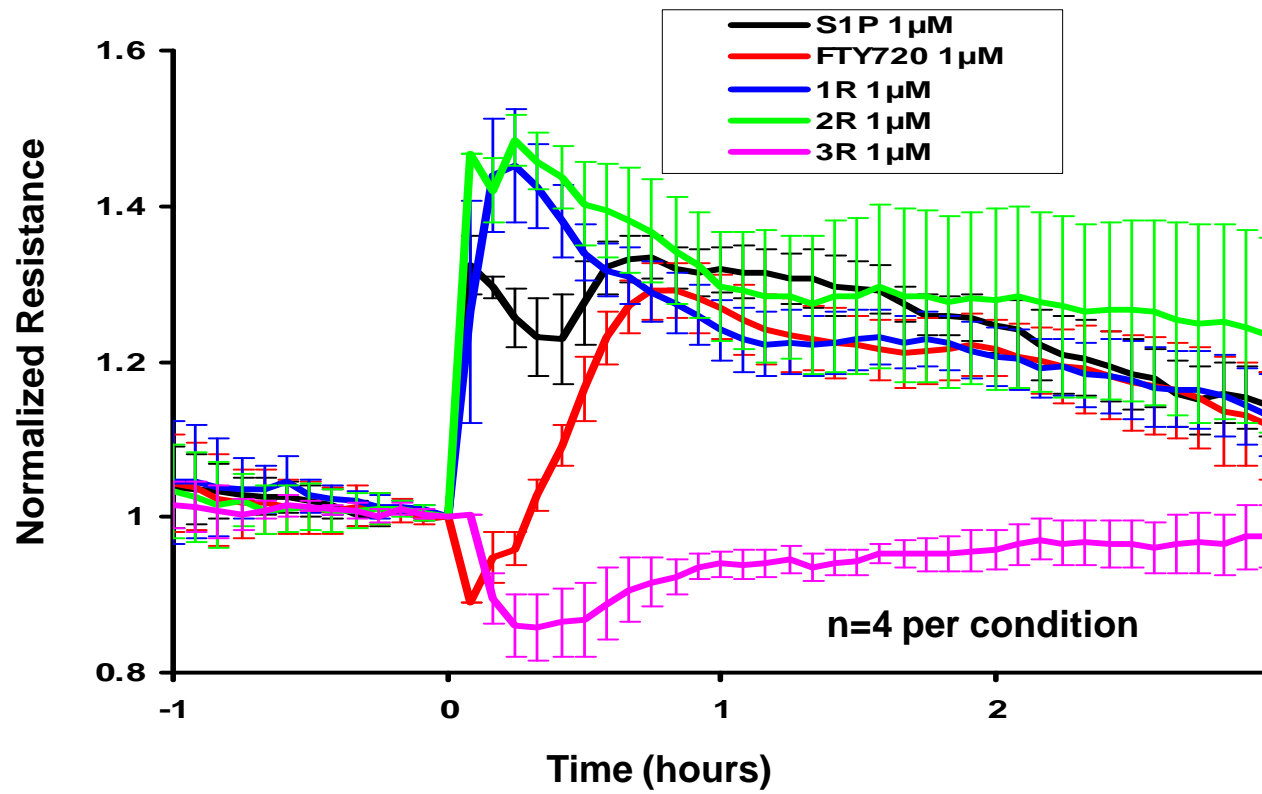


Figure 2b

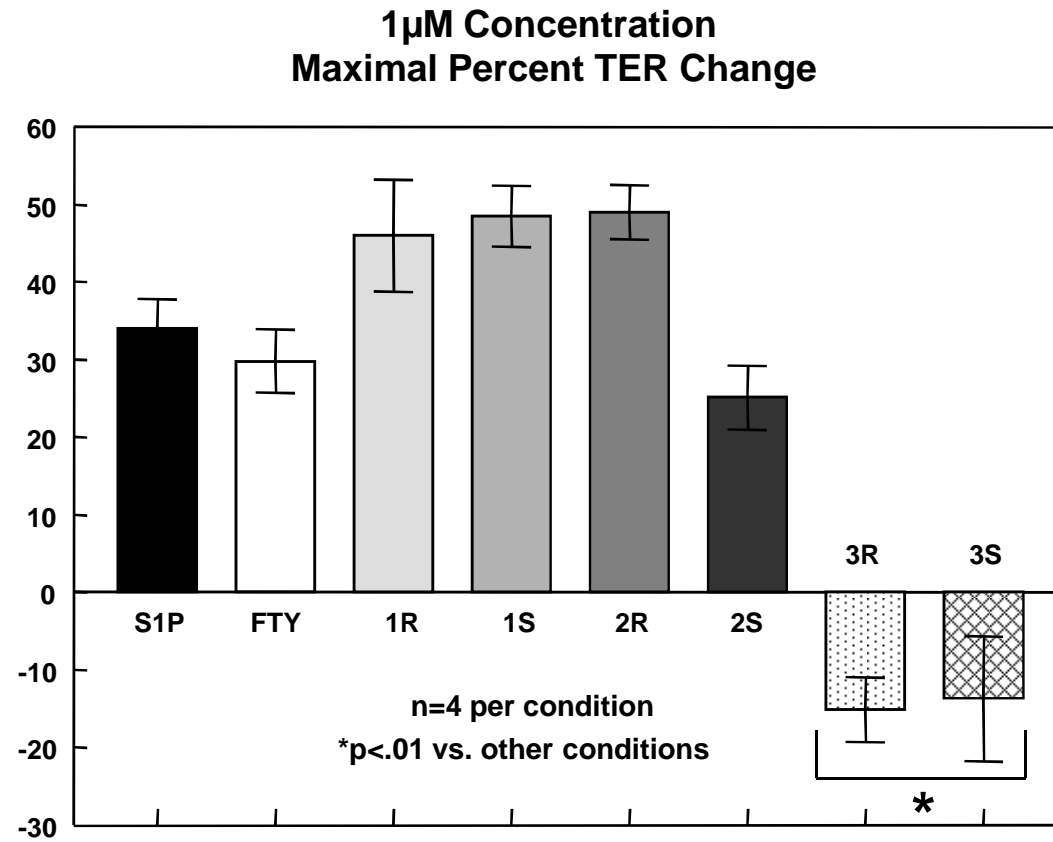


Figure 2c

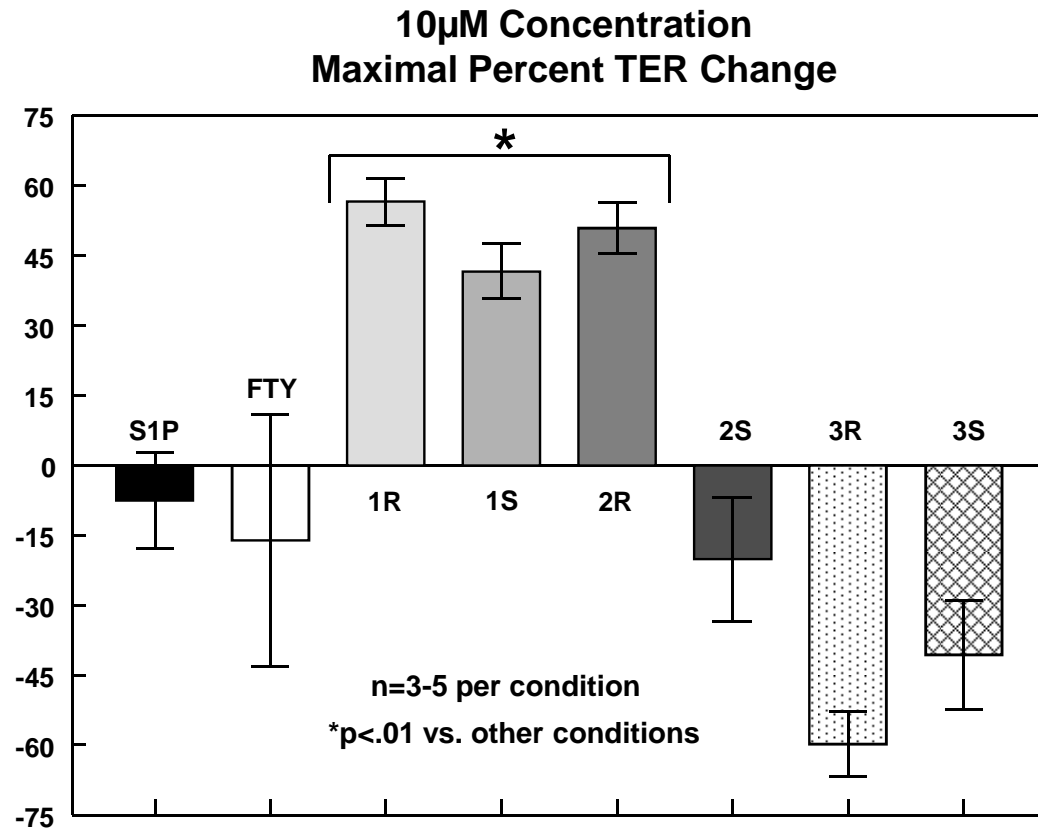


Figure 3

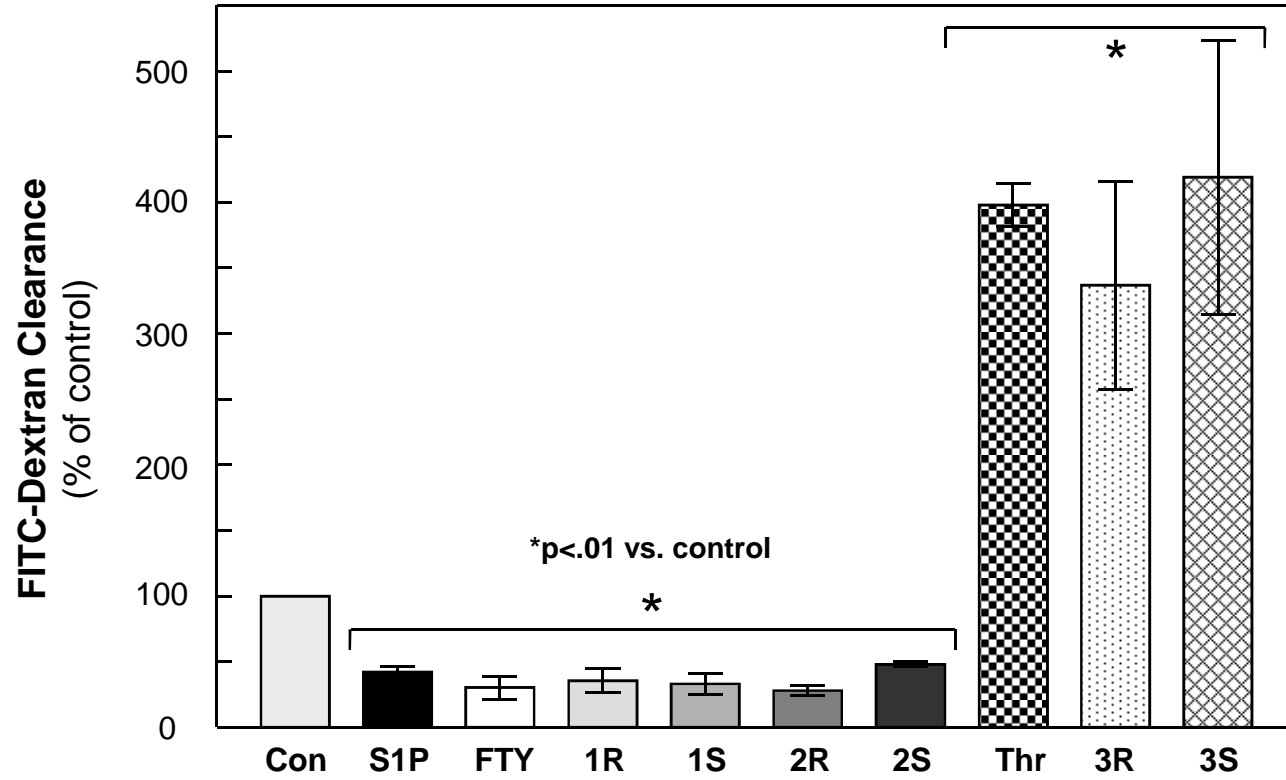


Figure 4a

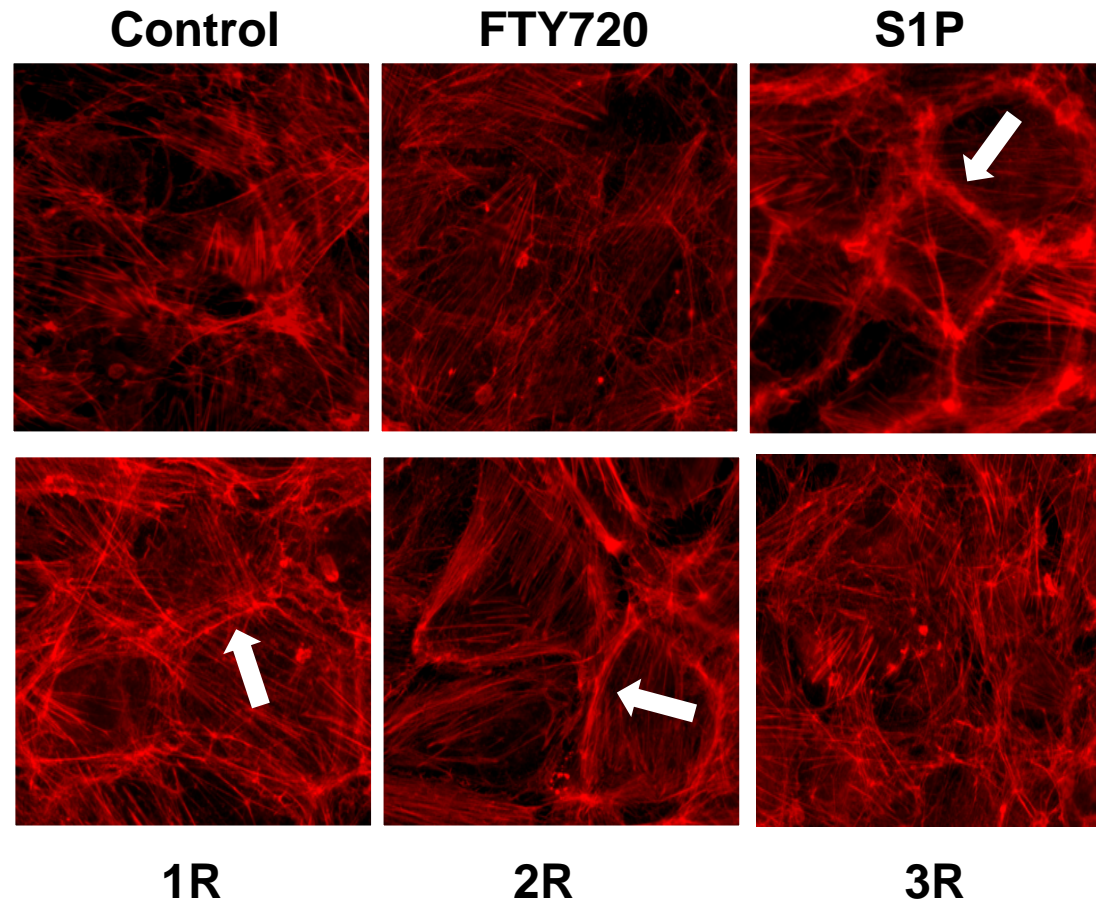


Figure 4b

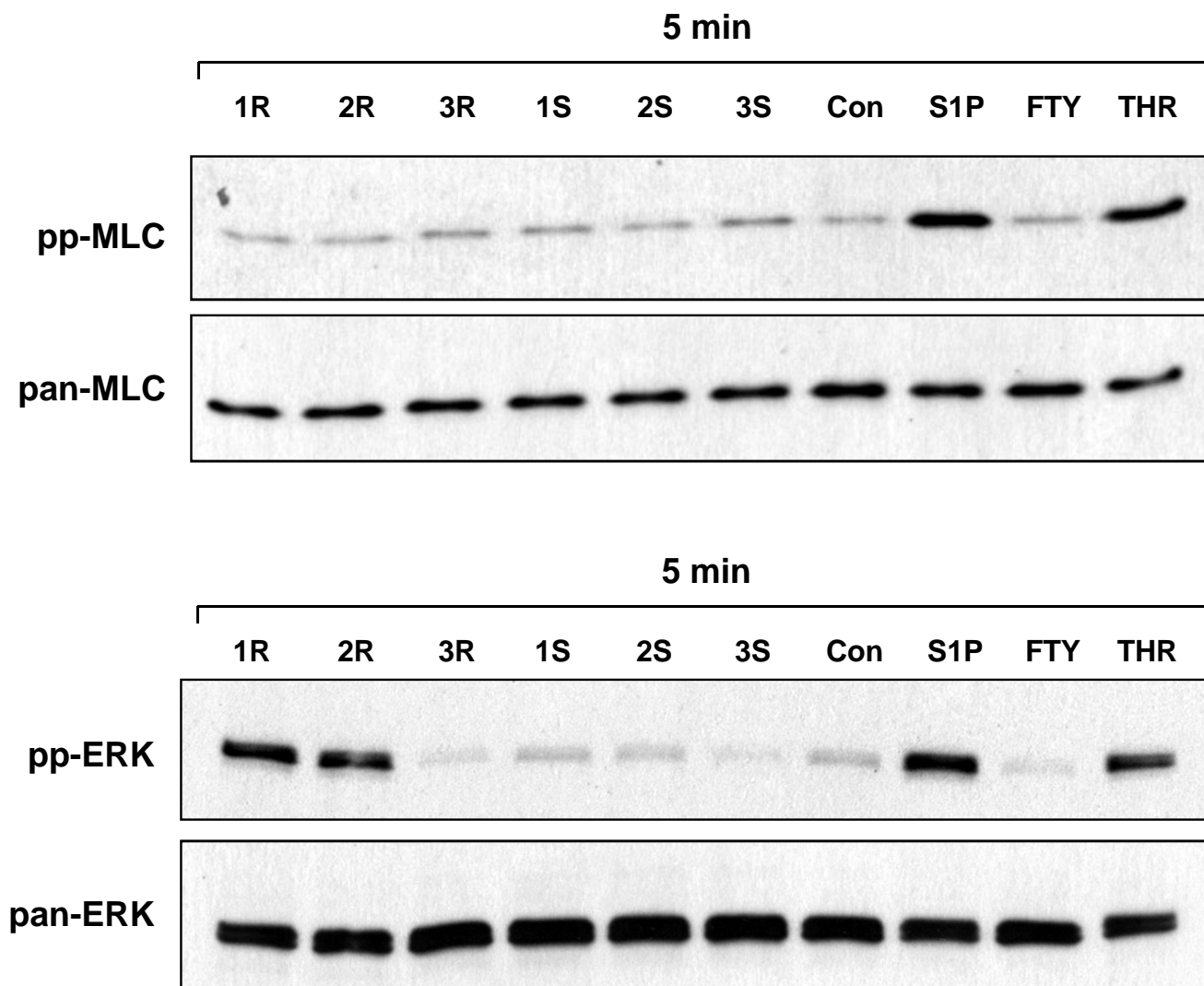


Figure 5

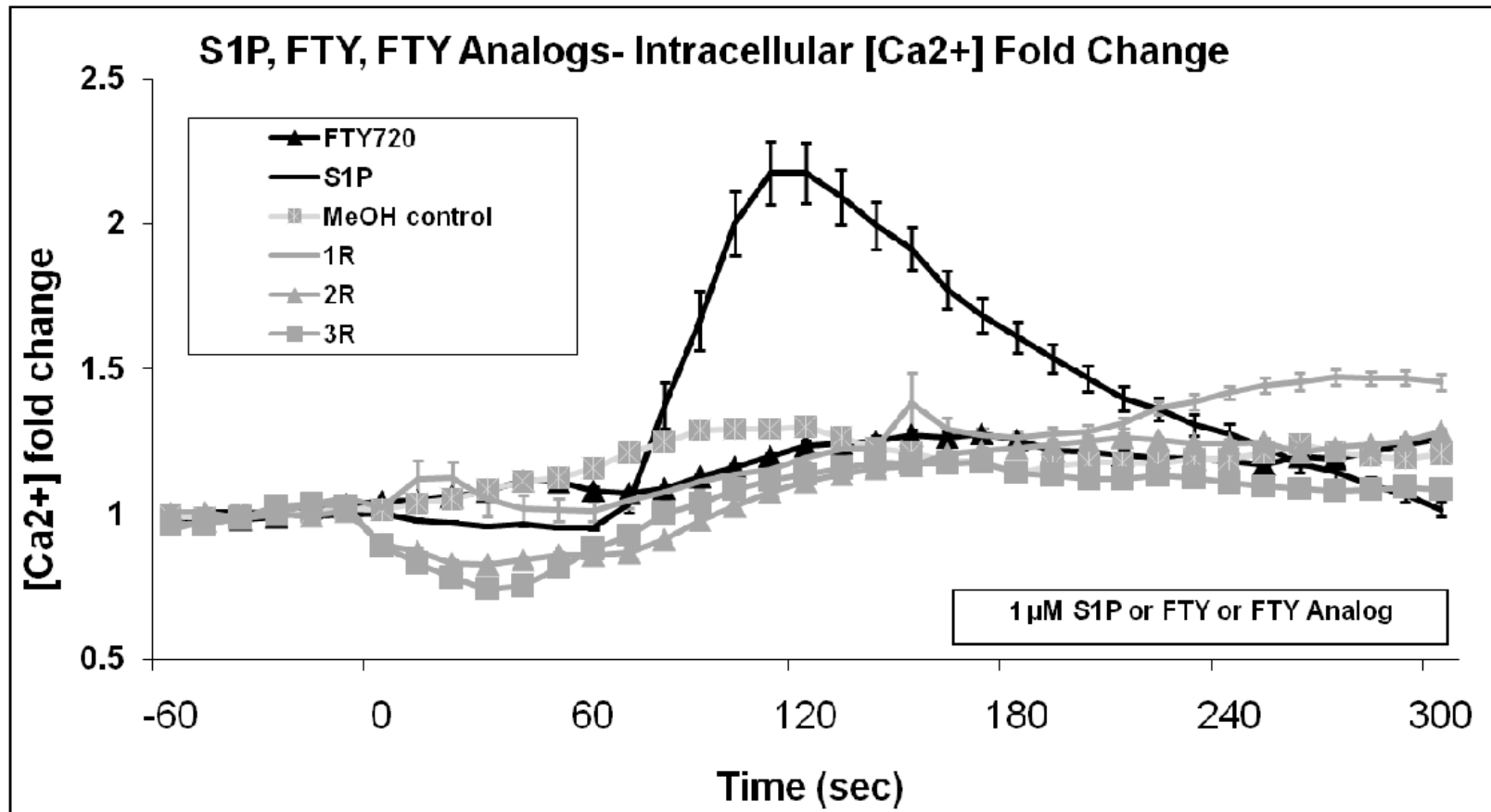


Figure 6a

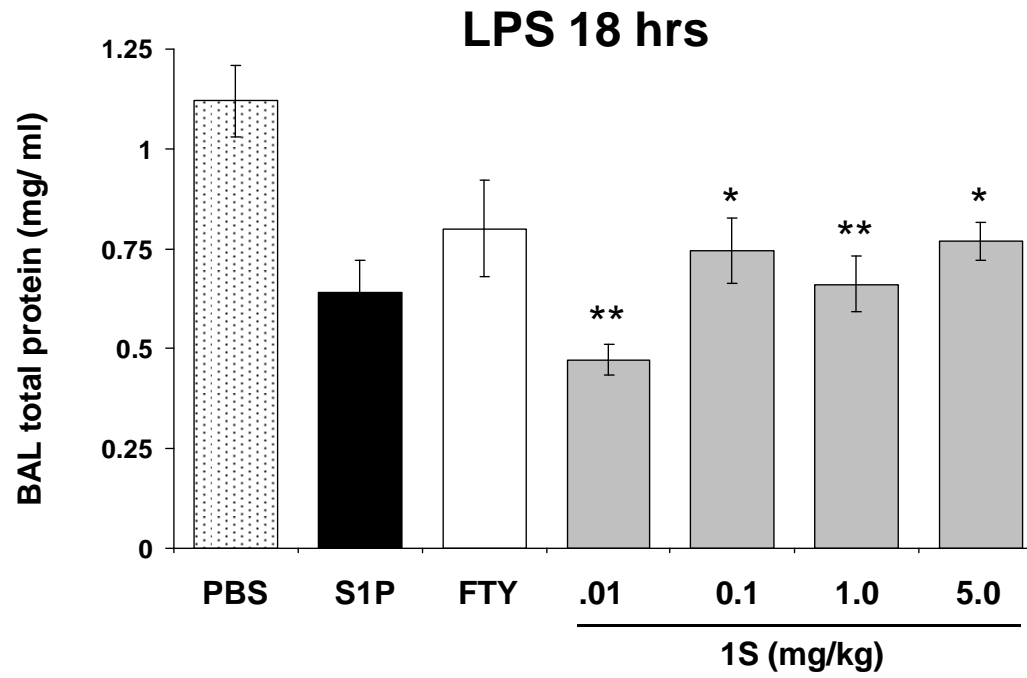
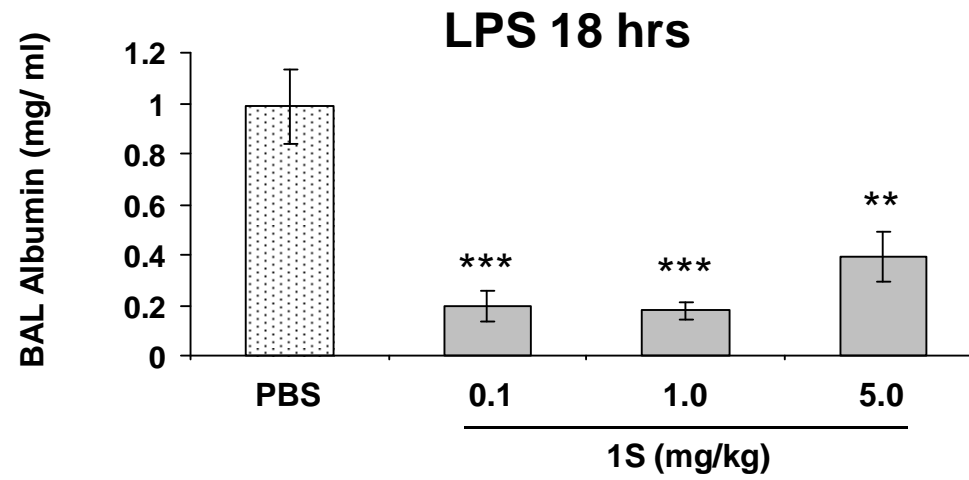


Figure 6b-c

B



C

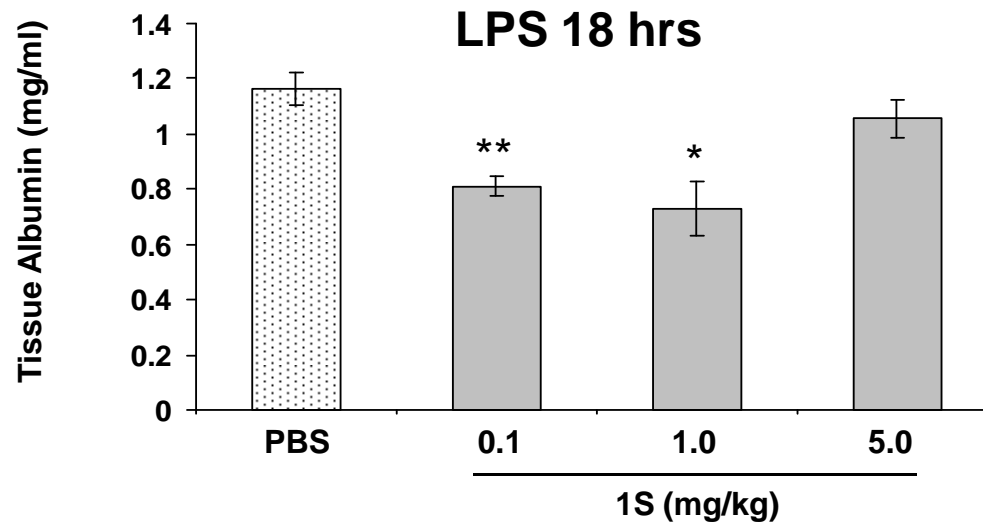


Figure 7

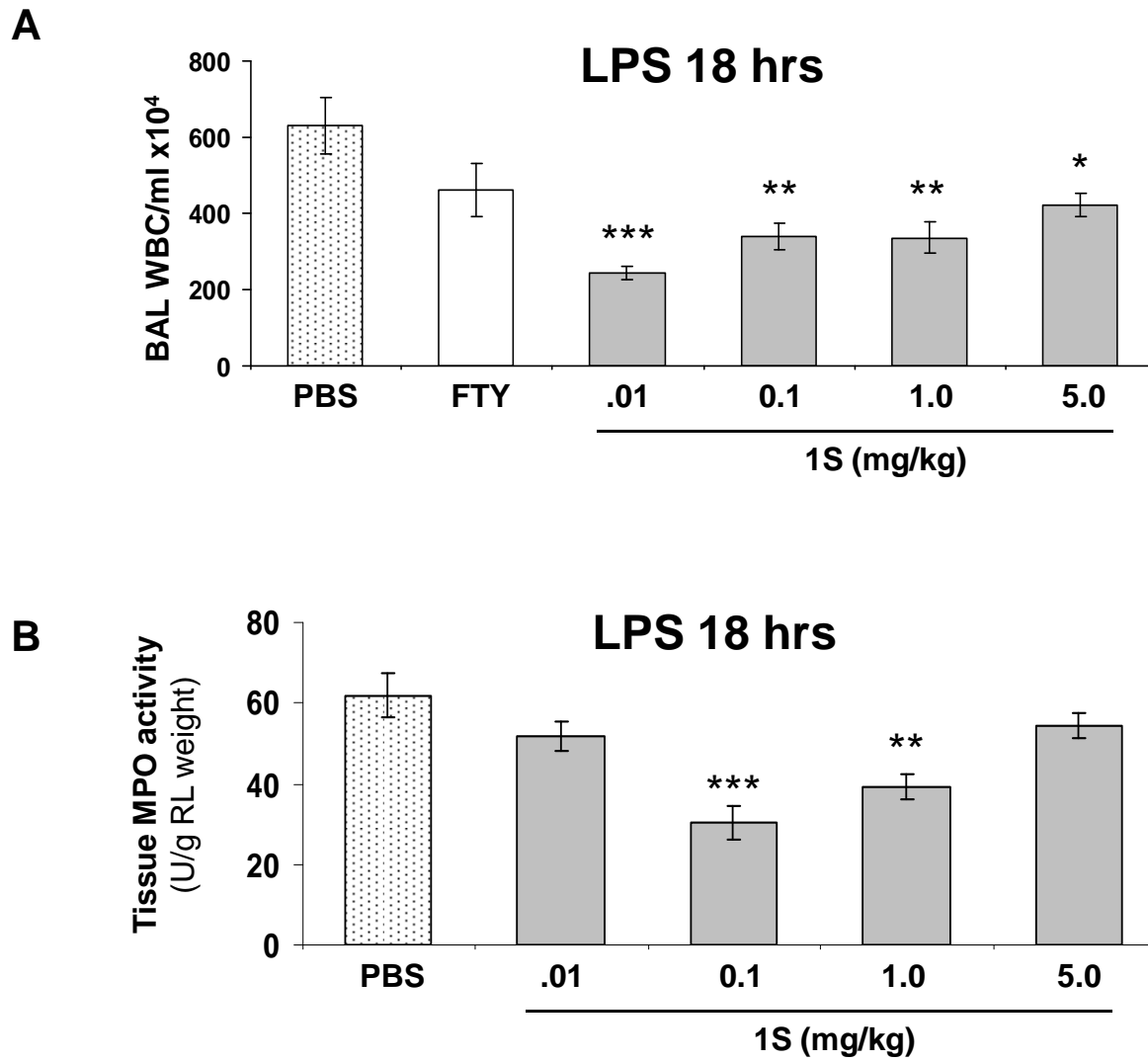


Figure 8

